A multiple hypotheses framework to study movement ecology and diet in a migratory songbird

Andrea Contina[1,†] Allison K. Pierce[1,*], Scott W. Yanco[1,*], Eli S. Bridge[2], Jeffrey F. Kelly[2,3,4], Michael B. Wunder[1]

[1] University of Colorado Denver, Department of Integrative Biology, Science Building 2074, Denver, CO 80217, USA

[2] Oklahoma Biological Survey, University of Oklahoma, 111 East Chesapeake Street, SC Building 134, Norman, OK 73019, USA.

[3] Corix Plains Institute and Department of Biology, University of Oklahoma, Five Partners Place, 201 Stephenson Parkway, Norman, OK 73019, USA

[4] Department of Biology, University of Oklahoma, 730 Van Vleet Oval, Norman, OK 73019, USA

* Denotes equal contribution

† Corresponding author's email: andrea.contina@ucdenver.edu

Abstract

Whether and how migratory organisms exhibit inter-individual behavioral and/or physiological variation across movement strategies remains an open question. The Dark-eyed Junco (*Junco hyemalis*) is a migratory songbird known for its intra-species variation displayed in relation to morphology, song repertoires, and migration. Thus, studies focusing on juncos can reveal how migratory strategy may covary with other individual-scale factors and, therefore, identify the selective forces driving intra-species variations throughout its distribution. We used Dark-eyed Junco hydrogen stable isotope feather values (δ^2H) and implemented a Bayesian framework to infer the breeding and molting origin of migratory juncos captured on their winter grounds in Oklahoma, United States (U.S.). We modeled the distribution of feather hydrogen stable isotope values as a function of five morphological variables including body mass and fat deposition measured in Oklahoma during the winter. We then investigated the trade-off between longer and more energetically costly migration strategies in relation to diet preferences through carbon ($\delta^{13}C$) and nitrogen ($\delta^{15}N$) stable isotope analysis from feather values. Dark-eyed Juncos wintering in south central U.S. likely originate from multiple breeding populations in northern U.S. and Canada. Body condition at the wintering ground (e.g., mass) had no effect on feather hydrogen stable isotope abundance. However, we found a positive correlation between nitrogen and hydrogen stable isotopes, suggesting that a trophic level shift towards insect consumption might occur in individuals migrating from southern latitudes. Increased insect-derived protein consumption might be explained by reduced fatty-acid reserves necessary to complete a shorter migratory journey.

Keywords: Stable isotope, hydrogen, avian migration, posterior probabilities, linear models

Introduction

Animal migration is a multifaceted life-history trait that evolved across taxa through complex behavioral and physiological adaptations (Alerstam and Bäckman, 2018). Migratory species maintain energetic balance between fuel consumption (e.g., fatty acid catabolism) and replenishing resources to effectively perform a long-distance migration (Guglielmo, 2018). However, research into how migrants sustain themselves during migration remains particularly challenging due to the small body size of many migratory songbirds and the fact that they travel, in some cases, thousands of kilometers per day (Rani et al., 2017; DeLuca et al., 2015). Species have developed unique behavioral strategies associated with seasonal movements (Horton et al., 2016), which depend on resource availability and seasonal environmental stochasticity. Thus, an understanding of these strategies requires examination of fluctuations in body mass and fat deposition in conjunction with behavior across the spatial extent of the species' distribution. This is relevant because variation in migration and foraging behavior at the intra-species level can place different evolutionary pressures on individual physiology and act as selective forces across populations. That is, there might be a trade-off between longer and more energetically costly migratory routes, potentially resulting in decreased body condition, and alternative strategies involving diet changes or morphological adaptations (e.g., longer or pointed wings) to accommodate the increased energetic demands of their migratory journey (Kaboli et al, 2007; Reif et al., 2016).

A suitable study system for disentangling different migratory strategies from other key evolutionary adaptations is offered by the Dark-eyed Junco (*Junco hyemalis*), a migratory songbird comprising numerous subspecies broadly distributed across North America. It is found breeding and molting in the northern regions of Canada and Alaska, and mountainous regions of

the United States (U.S.) and wintering in the lower latitudes of Canada and the majority of the continental U.S. and northern Mexico (Nolan et al., 2002). This species has shown negative population trends of over 40% in some areas in the last decade (PIF 2017; Rockwell et al., 2019) and its physiology and migratory behaviors have been the focus of numerous studies (Nolan and Ketterson, 1983; Rogers et al., 1994.; Fudickar et al., 2016; Liebgold et al., 2019).

Bridge et al. (2010) analyzed hydrogen isotope ratios from secondary feathers in a population of Dark-eyed Juncos, all from the same *hyemalis* subspecies group (slate-colored), sampled during the winter of 2009 in central Oklahoma (U.S.) and showed isotopic variation ranging from -175.6‰ to -118.6‰ from Vienna Standard Mean Ocean Water (VSMOW). This large range of variation (~60‰) in hydrogen stable isotope values prompted the authors to speculate that individuals from a wide geographic range of breeding, and consequently molting, locations wintered in Oklahoma, although the study did not include explicit probabilistic geographic assignments of wintering individuals, nor did it consider their variation in trophic level.

Although the subspecies of Dark-eyed Junco's are primarily differentiated by morphology and/or geographic distribution, considerable behavioral diversity between and even within subspecies presents a unique opportunity to address large-scale spatial and ecological hypotheses. For example, we argue that among different geographic populations that converge on a common wintering location, we should expect to observe variance in body condition during the time post-arrival or evidence of diet differences to accommodate the physiological demands of longer or shorter migration distances. One possibility is that long-distance migrants would have a lower body mass than short-distance migrants during the post-arrival period (e.g., first 6 weeks) due to the increased energy requirements of a longer journey (Fig 1 – panel A). This

outcome would be especially likely if individuals migrate directly from northern latitudes without utilizing stopover sites, such that they bear the costs of migration all at once (Cooper et al., 2015). However, if birds from more northerly breeding grounds are larger than their southern counterparts then effects on body mass could be masked—*i.e.*, larger birds from the north could appear of similar body mass during the post-arrival time window at the wintering site as smaller birds that flew shorter distances (Fig 1 – panel B). There might also be no discernable differences in body mass among long– and short– distance migrants if long–distance migrants adopt a movement strategy that includes frequent stopover refueling between the breeding and wintering grounds (Alerstam, 2011; Fig 1 – panel C).

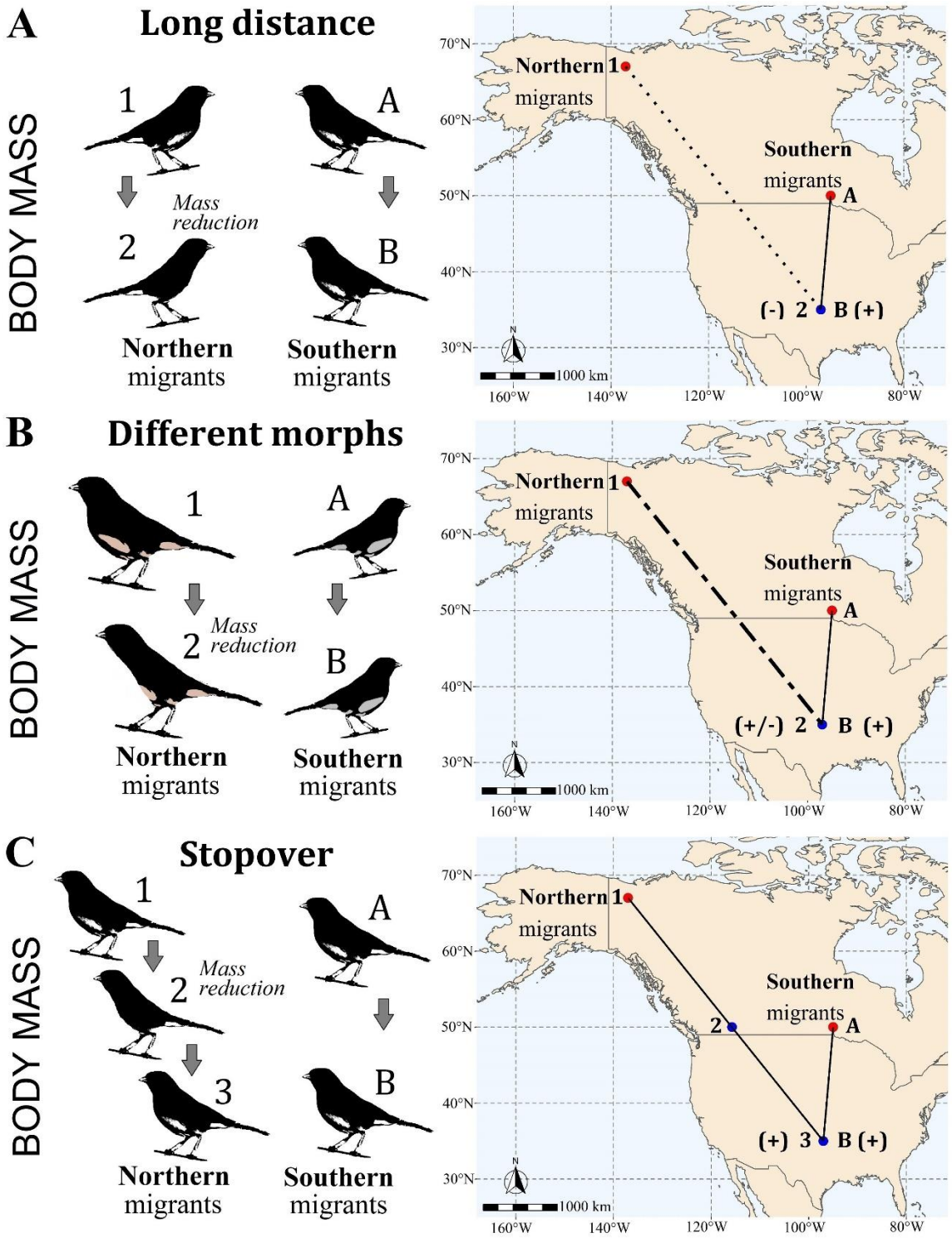

Figure 1. Heuristic working hypotheses showing different migration scenarios leading to potential effects and confounds in predictive models. Panel A: Long-distance migrants arrive with low body mass (indicated by a 'minus' sign) relative to short distance migrants (indicated by a 'plus' sign). Panel B: Body masses converge on the wintering grounds as larger migrants from the north lose more mass than

smaller, short distance migrants. Panel C: Long-distance migrants refuel in route such that they arrive on the wintering grounds with body masses similar to those of short-distance migrants.

To evaluate these alternative scenarios, we used hydrogen stable isotope data to estimate breeding location origins of a population of Dark-Eyed Juncos wintering in Oklahoma, and we collected a suite of morphological measurements after the birds completed fall migration. We reasoned that if there are different morphs of *J. hyemalis* originating from a wide range of latitudes admixing in Oklahoma over the winter, northern birds performing a longer and more energetically costly migration would either show (i) similar body mass if characterized by a larger body size compared to southern *J. hyemalis* or (ii) reduced body mass due to higher energetic expenditure. If, after controlling for body size, birds originating from different breeding grounds and wintering at the same site in Oklahoma show indistinguishable body mass, then we hypothesize that (iii) a rapid physiological mechanism in conjunction with available food resources must take place within the first few weeks upon arrival to attenuate body mass differences. Finally, we predict that Oklahoma wintering birds originating from northern latitudes would have (iv) a higher carbohydrate intake, but lower protein consumption compared to wintering birds from southern latitudes due to their need to fuel a longer migratory journey. To test this last hypothesis, we assessed pre-migratory diets by examining carbon and nitrogen stable isotope ratios in flight feathers. In addition to quantifying geographic connectivity apparent in the admixture of a Dark-eyed Junco wintering population, this study offers new insights into how this species negotiates tradeoffs between migration distance and maintenance of body mass. Importantly, we present a multiple working hypotheses framework (Yanco et al. 2020) to identify possible confounding effects in explanatory models for different migration strategies across populations.

Methods

Study Area

We studied Dark-eyed Juncos wintering in central Oklahoma where the species forages in open woodland habitats and feeds on grass sprouts, *Taraxacum* sp. and various species of insects (Bridge et al. 2010). The weather conditions during our study (January and February 2009) as recorded by the Oklahoma Climatological Survey and the Oklahoma Mesonet (www.mesonet.org) at the Norman (NRMN) weather station indicated monthly average temperature ranging from 2.7 to 8.9 °C, monthly average precipitation ranging from 22.8 to 24.6 mm, and monthly average wind speed ranging from 15.6 to 18.1 kph. Detailed winter data from the NRMN weather station are presented in the supplementary material (Table S1).

Sample collection and stable isotope analysis

We used published hydrogen stable isotope data from 80 Dark-eyed Junco sampled in central Oklahoma, USA (35°10' N, 97°26' W) during winter 2009 (Bridge et al. 2010). After removing individuals with missing capture information, our data set comprised hydrogen stable isotope values of secondary feathers from 76 migrants that we used to infer geographic breeding and molting origin. We also present novel carbon and nitrogen stable isotope data obtained from a subset (N = 74) of those migrants sampled in Oklahoma that we used to study habitat use and trophic level. However, after filtering out individuals with missing morphometric measurements we had data from 62 migrants (39 adult males and 23 adult females) that we used for morphological models. All samples were collected between January and February of the same year. Feathers were prepared for analysis of stable isotope ratios of hydrogen (δ^2H), carbon ($\delta^{13}C$), and nitrogen ($\delta^{15}N$) by following standard washing protocol in a 2:1 solution of

chloroform-methanol to remove debris and oil contaminants (Paritte and Kelly 2009). Samples for hydrogen stable isotope ratios analysis were processed through a Thermo-Finnigan Delta V isotope ratio mass spectrometer interfaced with a high-temperature pyrolysis elemental analyzer (TC/EA, Thermo-Finnigan, Bremen, Germany). Feather δ^2H values (δ^2H_f) are reported as mean ± SD in delta notation of parts per mil (‰) from the standards ($\delta D_{sample} = [(R_{sample}/R_{standard}) - 1] \times 1{,}000$) compared to the Vienna Standard Mean Ocean Water (VSMOW). We used chicken feather standard (CFS; -147.4‰), cow hooves (CHS; -187‰), and bowhead whale baleen (BWB; -108‰) as keratin which are widely adopted for sample comparative equilibration (Wassenaar and Hobson, 2003). The details of hydrogen sample measurement are in Kelly et al. 2009. We conducted carbon and nitrogen stable isotope ratios analysis on a Thermo-Finnigan DeltaPlus isotope ratio mass spectrometer connected to a Carlo Erba elemental analyzer. We normalized the $\delta^{13}C$ and $\delta^{15}N$ samples to the Vienna Pee Dee Belemnite (VPDB) and AIR scales, respectively, and used Brown-headed cowbird (BHCO; *Molothrus ater*) feather standards. The values of $\delta^{13}C$ and $\delta^{15}N$ standards were -15.7 ± 0.1‰ ($\delta^{13}C$ BHCO), and 7.6 ± 0.1‰ ($\delta^{15}N$ BHCO).

Feather Calibration and Geographical Assignments

We implemented a Bayesian analytical framework in the R package assignR to spatially reconstruct juncos' breeding and/or molting areas (Ma et al., 2020; R Core Team, 2020). First, we rescaled precipitation isotope values (δ^2H_p) from a North America geostatistical model (Bowen et al. 2005) to 22 known-origin Song Sparrow (*Melospiza melodia*) samples provided by Hobson et al. (2012) and Hobson and Koehler (2015). To ensure a more accurate isotopic calibration (Wunder 2010), we used linear regression to model mean tissue isotope values as a

function of precipitation isotope values using the *calRaster* function in assignR. We recognize that a species-specific calibration provides higher degree of accuracy. However, when species-specific known-origin tissues are not available, calibration data from closely related species can be used (Hobson et al., 2012). Our data set comprised entirely unknown-origin feather samples from Dark-eyed Juncos; therefore, we used published data of *M. melodia*, a species of comparable size, diet, and spatial distribution (Arcese et al., 2002; Hobson et al., 2012).

We determined the molting locations of juncos wintering in Oklahoma by computing posterior probability density maps through the *pdRaster* function in assignR (Wunder 2010; Ma et al., 2020). We present normalized posterior probability maps representing both the individual and cumulative group probabilities of origin from each grid cell restricted to the breeding and year-round distribution ranges (BirdLife International 2016). To visualize the cumulative group probabilities of origin, we clustered the samples into four isotopic groups based on the reported stable isotope feather values (δ^2H_f) across the junco data set arranged from the lowest values (G1) to the highest values (G4): the first group (G1) included δ^2H_f values ranging from -175.6‰ to -160.2‰ (M = -167.1‰, SD = 5.02‰, N = 18); the second group (G2) included values ranging from -159.3‰ to -150.4‰ (M = -154.9‰, SD = 3.17‰, N = 23); the third group (G3) included values ranging from -149.8‰ to -140.1‰ (M = -145.4‰, SD = 2.88‰, N = 19); and the fourth group (G4) included values ranging from -139.3‰ to -118.6‰ (M = -130.4‰, SD = 6.39‰, N = 16). Even though this clustering approach is *ad hoc*, it still represents a useful subdivision based on δ^2H_f variation across birds in our dataset. Wassenaar and Hobson (2006) estimated that ±3‰ variation in hydrogen stable isotope extracted from feathers translates approximately to 1 degree of latitude (or ~111 km). Therefore, the differential range of about 10‰ or more that we used to cluster birds into four groups corresponds to ~370 km of

geographic separation (Hobson and Wassenaar, 1996; Wassenaar and Hobson, 2006). This distance is presumably large enough to consider our samples from different breeding populations.

Modeling morphometric parameters

We investigated the effect and relative predictive importance of five different morphometrics on mean hydrogen stable isotope ratios in Dark-eyed Junco feathers (δ^2H_f). Our explanatory variables were: wing chord (mm), tarsus length (mm), tail length (mm), mass (g), and fat depositions scored on a six-point ordinal scale (Helms and Drury 1960). We did not include body mass index normalized by a structural measure because this would be collinear with other included variables and additive model combinations should account for size normalized mass (Green, 2001). We controlled for morphological variance across males and females by including 'sex' as a random effect in all our models and to standardize evaluation of predictive influence between the morphometric variables measured on different scales we Z-scored values for all variables. We modeled a complete combinatorial set of linear models in the R package MuMIn (Barton and Barton, 2019) and computed the relative importance of individual morphometric variables through a variable importance analysis using Akaike Information Criterion corrected for small sample sizes (AICc) summed model weights for each model containing a given variable. We then compared the sum of all the AICc weights and odds ratios to evaluate the relative importance of each variable.

Trophic Level Analysis

We analyzed stable carbon ($\delta^{13}C$) and nitrogen ($\delta^{15}N$) isotopes in feather samples to explore trophic level partition among birds migrating from northern and southern latitudes as revealed by hydrogen ($\delta^{2}H$) data. We exploited the occurrence of distinct plant photosynthetic pathways, knowing that trees and shrubs in temperate climates (e.g., C3 plants) are depleted in carbon compared to plants inhabiting arid environments and adopting C4 or CAM photosynthesis (Keeley and Rundel, 2003). These differences help to assess the proportion of proteins deriving from C3 and C4 plants, while higher nitrogen values indicate a shift towards a diet less dependent on seeds and richer in insects. Thus, we used the *corr.test* function in the R package psych (Revelle and Revelle, 2015) to perform a Pearson correlation test between carbon ($\delta^{13}C$) and hydrogen ($\delta^{2}H$) and between nitrogen ($\delta^{15}N$) and hydrogen ($\delta^{2}H$) stable isotopes. This test highlights diet trends in relation to latitudinal origin as determined by $\delta^{2}H$ data. We then used the *levelplot* function in the R package lattice (Sarkar 2008) to create a visual representation of $\delta^{2}H$ values from feathers collected in Oklahoma and their distribution within the sampling space.

Results

Rescaling model and posterior probability density maps

The rescaling model provided a robust relationship between precipitation isotope values ($\delta^{2}H_{p}$) and known-origin samples of the species *M. melodia* ($y = -35.08 + 0.91x$; $R^2 = 0.79$, $CI_{95\%}$ [0.74, 0.95], n = 22) and allowed us to calibrate our isoscape to determine junco posterior probability of origin (Fig. 2 – panel A). We obtained a rescaled environmental isoscape raster of 52,884 cells at 0.33km resolution and a range of hydrogen stable isotope values spanning -193.3‰ and -41.3‰ (M = -122.9‰; SD = 37.2‰; Fig 2 – panel B and C).

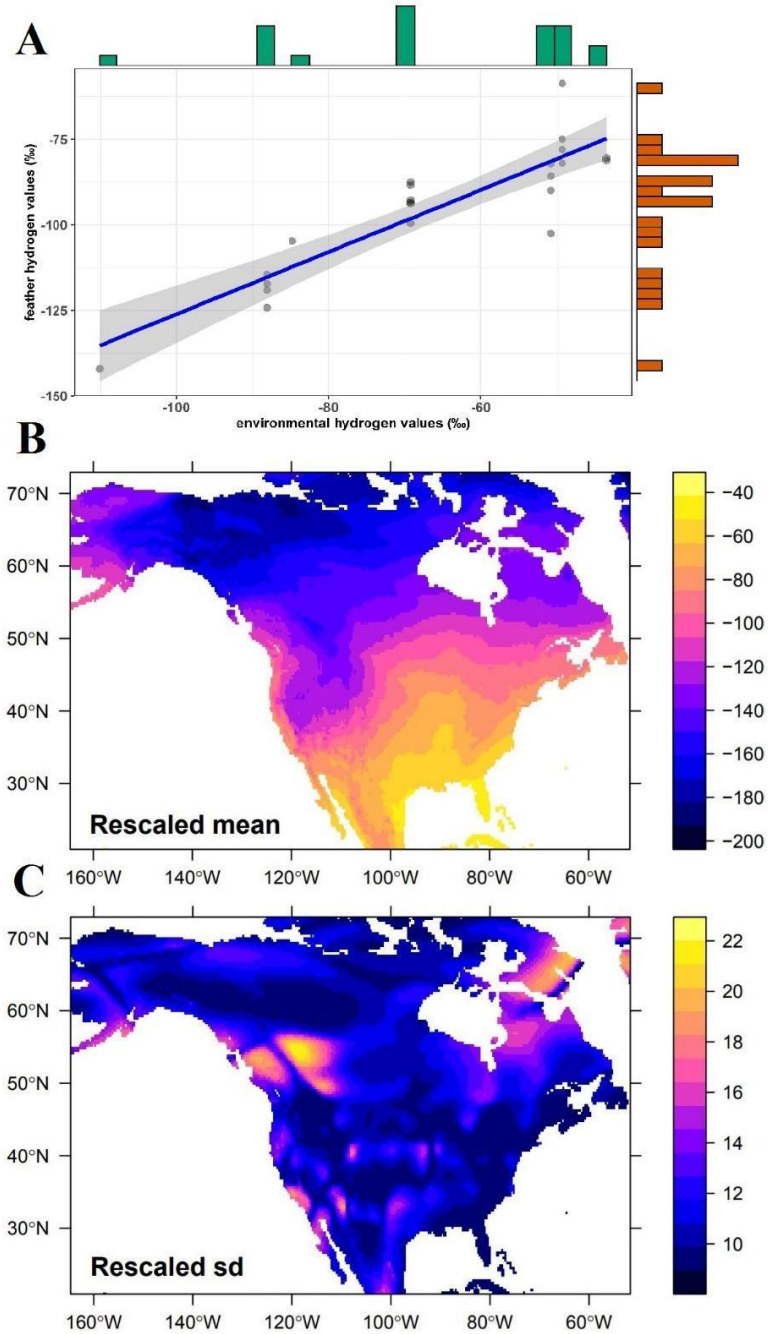

Figure 2. Linear regression model between environmental precipitation isotope values (δ^2H_p) and 22 known-origin feather samples of *M. melodia* samples (panel A) used to rescale the North America hydrogen isoscape (panel B and C) for assigning migratory juncos wintering in Oklahoma to their molting locations at the breeding grounds across northern United States and Canada. The green and orange bars along the horizontal and vertical axis represent the distributions of the sampling data across environmental and tissue isotope values, respectively (panel A). The calibrated hydrogen isoscape mean values and standard deviations are presented in panel B and C, respectively.

Once we performed isoscape tissue calibration, we inferred the spatial extent of the breeding and molting origin of 76 Dark-eyed Juncos wintering in Oklahoma through a Bayesian probabilistic framework. Our posterior probability density maps, either at the group (Fig 3) or individual level (supplementary material; S1-S4), show distinct latitudinal variation across the breeding and molting range of migratory juncos. Overall, the northernmost migrants were assigned to either Alaska and western Canada, including Yukon Territory and British Columbia, or central Northwestern Territories, while southern migrants were assigned to either Northern Saskatchewan or southern Manitoba and northwestern United States near the Rocky Mountains. However, even though the probability assignment surfaces for the southern migrants (group G3 and G4) were largely distributed at latitudes lower than 60°N (Fig. 3), we also found weak probabilities of origin along the western coast of Alaska due to the underlying structure of the precipitation isoscape used for rescaling (Fig 2, panel B-C; Fig S3 and S4). Taken together, these results suggest that different Dark-eyed Junco populations admix into the same wintering area in central Oklahoma.

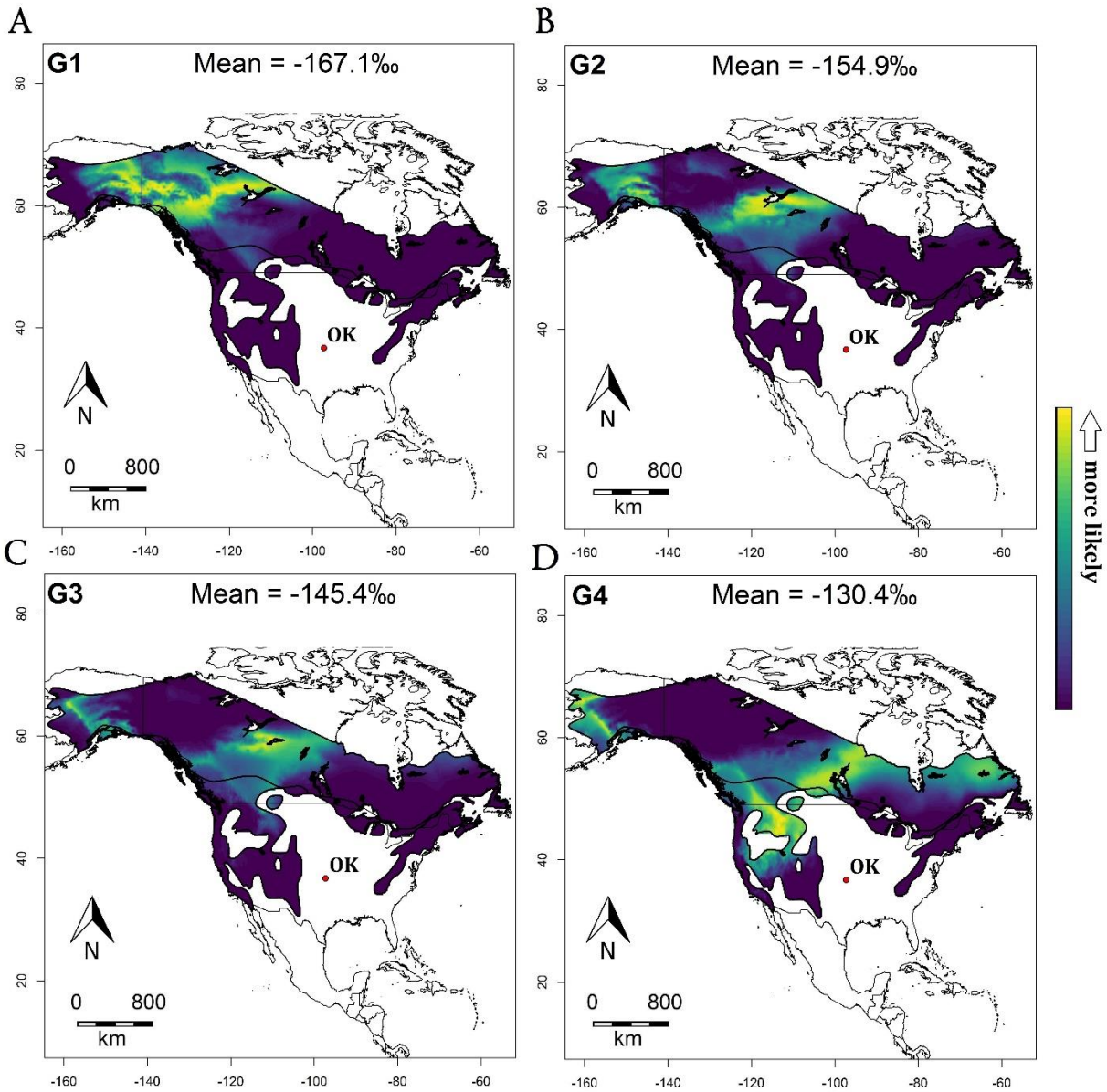

Figure 3. Cumulative assignment posterior probability density maps across four isotopic groups of 76 Dark-eyed Juncos wintering in Oklahoma (red dot) and breeding at northern latitudes in the United States and Canada. The bright yellow color represents high probabilities of molting origin. The northern migrants (groups G1 and G2; panel A and B) were assigned to either Alaska and western Canada, including Yukon and British Columbia, or central Northwestern Territories. The southern migrants (groups G3 and G4; panel C and D) were prevalently assigned to either Northern Saskatchewan or southern Manitoba and northern western United States. The hydrogen stable isotope approach suggests that Dark-eyed Junco migrants from different breeding populations converge into the same location in Oklahoma over the winter.

Variable importance analysis

The analysis of the importance of variables revealed no clear predictive support for any variable considered in our models. We fit a full set of 32 linear mixed-effect models for mean δ^2H_f including single variable models and all the possible combinations of the five predictors, with a random effect of sex and ranked them using Akaike Information Criterion corrected for small sample size (AICc). All 5 variables we considered had relatively high summed AICc evidence weights suggesting models containing each respective variable outperformed those that did not (Table 1 and Table 2). Fat score had the highest summed AICc weight value and odds ratios, indicating that models containing the fat score variable accounted for all of the weight of AICc values for the model set (Table 1). However, the estimated effect of fat score on mean δ^2H_f was indistinguishable from 0 in all models weighted by AICc (Table S2, Figure 4A) suggesting that despite being the most comparatively informative variable, it had no discernible effect on δ^2H_f values in our data set. Similarly, estimates for other variables we considered also lacked support for non-zero effects (Table S2, Figure 4B).

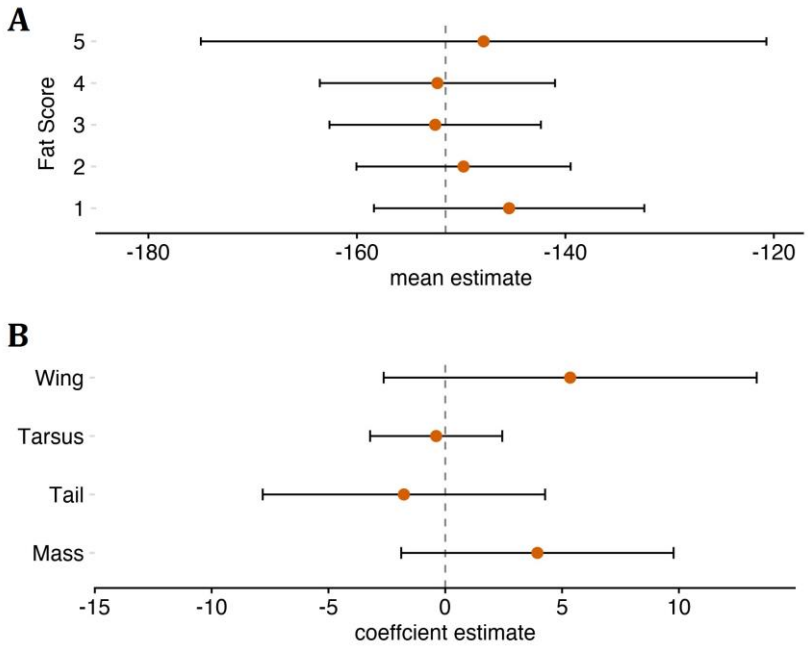

Figure 4. Model averaged estimates of mean δ^2H_f values with 95% CI for levels of fat scores with centered and scaled morphometric metric measures held at 0, their mean value (A) and model averaged coefficient estimates of centered and scaled morphometric parameters with 95% CI with level 1 of fat score as the reference for the intercept (B). Both plots indicate effects for fat scores and morphometric variables on mean δ^2H_f are insignificant for our data set as evidenced by CI overlap between fat score levels (A) and with zero (B).

Variable	Sum of AICc model weights	Odds ratio
Fat	1	inf
Mass	0.87	6.69
Wing	0.86	6.14
Tail	0.72	2.57
Tarsus	0.54	1.17

Table 1. Variable importance results. Although the variable 'body fat' emerged as the comparatively best predictor of hydrogen variation in feathers, the effect for this and all other variables could not be differentiated from zero.

Model ID	Model Variables	logLik	AICc	delta	weight
32	h ~ Fat + Mass + Tail + Tarsus + Wing + (1 | sex)	-222.1	471.48	0	0.3
24	h ~ Fat + Mass + Tail + Wing + (1 | sex)	-223.74	471.8	0.33	0.25
28	h ~ Fat + Mass + Tarsus + Wing + (1 | sex)	-224.61	473.54	2.06	0.11
20	h ~ Fat + Mass + Wing + (1 | sex)	-226.25	473.95	2.47	0.09
30	h ~ Fat + Tail + Tarsus + Wing + (1 | sex)	-225.43	475.16	3.69	0.05
22	h ~ Fat + Tail + Wing + (1 | sex)	-226.94	475.33	3.86	0.04
16	h ~ Fat + Mass + Tail + Tarsus + (1 | sex)	-225.65	475.61	4.13	0.04
8	h ~ Fat + Mass + Tail + (1 | sex)	-227.18	475.83	4.35	0.03
12	h ~ Fat + Mass + Tarsus + (1 | sex)	-227.46	476.38	4.91	0.03
4	h ~ Fat + Mass + (1 | sex)	-228.98	476.68	5.21	0.02
26	h ~ Fat + Tarsus + Wing + (1 | sex)	-227.69	476.85	5.37	0.02
18	h ~ Fat + Wing + (1 | sex)	-229.2	477.11	5.63	0.02
14	h ~ Fat + Tail + Tarsus + (1 | sex)	-229.25	479.96	8.48	0
6	h ~ Fat + Tail + (1 | sex)	-230.84	480.39	8.91	0
10	h ~ Fat + Tarsus + (1 | sex)	-232.01	482.74	11.26	0
31	h ~ Mass + Tail + Tarsus + Wing + (1 | sex)	-233.91	483.9	12.42	0
2	h ~ Fat + (1 | sex)	-233.92	483.91	12.44	0
23	h ~ Mass + Tail + Wing + (1 | sex)	-235.4	484.32	12.85	0
27	h ~ Mass + Tarsus + Wing + (1 | sex)	-236.3	486.13	14.66	0
19	h ~ Mass + Wing + (1 | sex)	-237.79	486.64	15.16	0
15	h ~ Mass + Tail + Tarsus + (1 | sex)	-237.14	487.81	16.33	0
29	h ~ Tail + Tarsus + Wing + (1 | sex)	-237.26	488.04	16.56	0
7	h ~ Mass + Tail + (1 | sex)	-238.62	488.32	16.84	0
21	h ~ Tail + Wing + (1 | sex)	-238.76	488.6	17.12	0
11	h ~ Mass + Tarsus + (1 | sex)	-238.93	488.93	17.45	0
3	h ~ Mass + (1 | sex)	-240.4	489.51	18.03	0
25	h ~ Tarsus + Wing + (1 | sex)	-239.41	489.89	18.41	0
17	h ~ Wing + (1 | sex)	-240.9	490.51	19.03	0
13	h ~ Tail + Tarsus + (1 | sex)	-240.75	492.58	21.1	0
5	h ~ Tail + (1 | sex)	-242.43	493.56	22.09	0
9	h ~ Tarsus + (1 | sex)	-243.45	495.6	24.13	0
1	h ~ (1 | sex)	-245.58	497.58	26.1	0

Table 2. Akaike Information Criterion corrected for small sample size (AICc) model selection results. The most parsimonious model was the full model including all five morphological variables but was equally competitive with a model omitting tarsus based on <2 unit difference in ΔAICc values. Simpler single term or intercept only models were generally outperformed by more complex models.

Migrant Diet Preferences and Trophic Level

The Pearson test did not identify a strong correlation between carbon ($\delta^{13}C$) and hydrogen ($\delta^{2}H$) isotopes values ($r = -0.17$, $p = 0.22$), but it suggested a moderately positive correlation between nitrogen ($\delta^{15}N$) and hydrogen ($\delta^{2}H$) isotopes values ($r = 0.33$, $p = 0.01$). These results suggest that a trophic level shift towards insect consumption might occur in migrants originating from lower latitudes (Fig. 5 panel A and B). Interestingly, when samples were grouped by wing length (Fig. 5 panel C and D), it appeared that birds with longer wings had a broader range of $\delta^{13}C$ values, indicating variability in their habitat use. Moreover, when plotting $\delta^{13}C$ against $\delta^{15}N$ over $\delta^{2}H$ feather isoscape within the sampling space, the changes in dietary niche across latitudinal origin appeared more evident (Figure 6 panel A-C; supplementary material; S5-S6). Northern migrants showed lower protein consumption ($\delta^{15}N$: 1-4‰) and C3-shrub habitat use ($\delta^{13}C$: -22 – -24‰), while southern migrants were characterized by a higher trophic level ($\delta^{15}N$: 4-8‰) and $\delta^{13}C$ towards C3-vegetation compatible with temperate forests ($\delta^{13}C$: -24 – -26‰). Analysis of diet preferences between sexes did not show marked differences, although males seem to have a slightly larger dietary niche compared to females (supplementary material; S7).

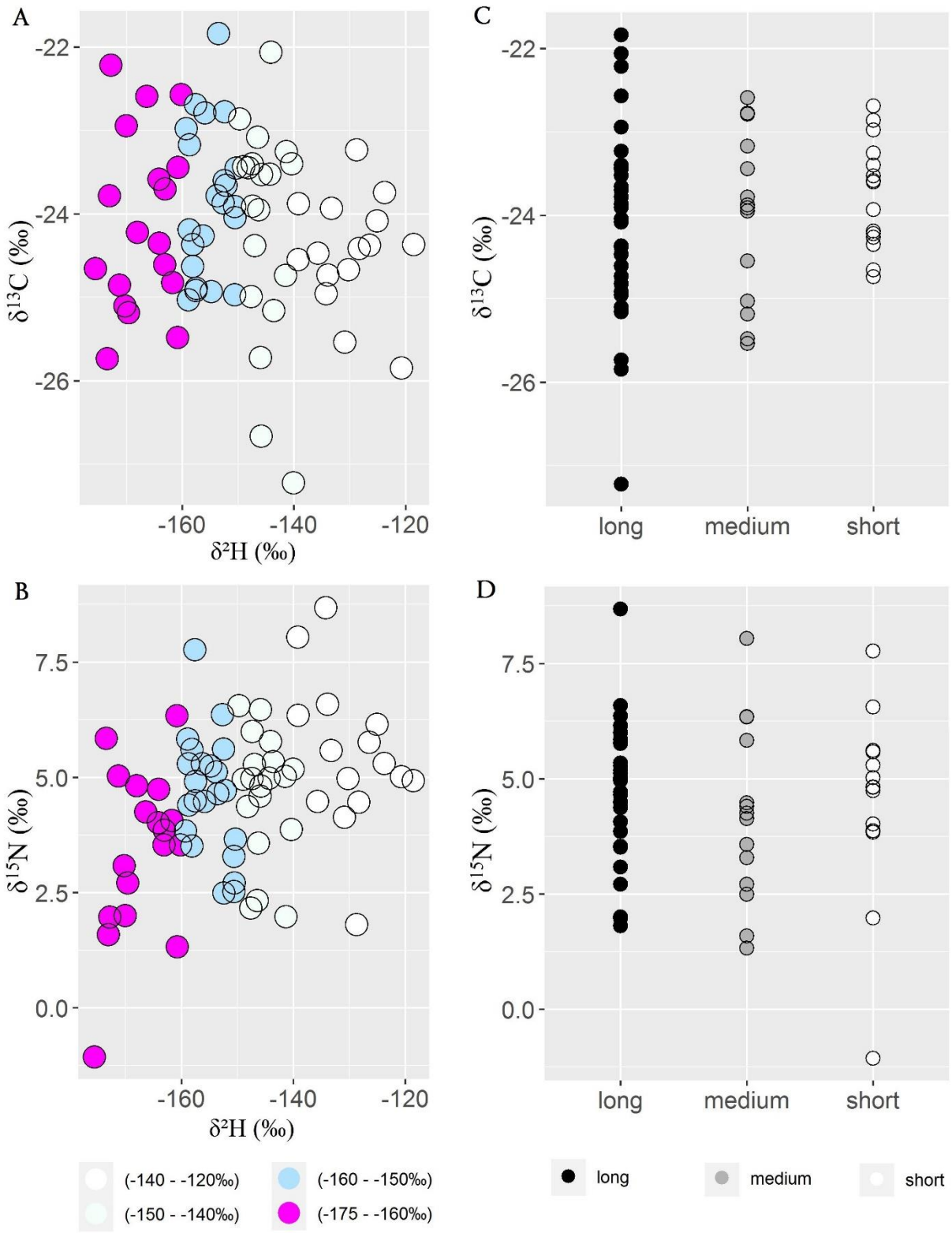
A
B
C
D
δ13C (‰)
δ15N (‰)
δ2H (‰)
-22
-24
-26
7.5
5.0
2.5
0.0
-160
-140
-120
long
medium
short
(-140 - -120‰)
(-150 - -140‰)
(-160 - -150‰)
(-175 - -160‰)

354

355

Figure 5. Correlation between $\delta^{13}C$ and hydrogen $\delta^{2}H$ (panel A) and nitrogen $\delta^{15}N$ and hydrogen $\delta^{2}H$ values (panel B). Migrants exhibiting longer wings show a broader range of $\delta^{13}C$ values compared to medium- and short-length wings birds suggesting more flexibility in their habitat use (panel C). We did not find noticeable trends between $\delta^{15}N$ and wing length (panel D).

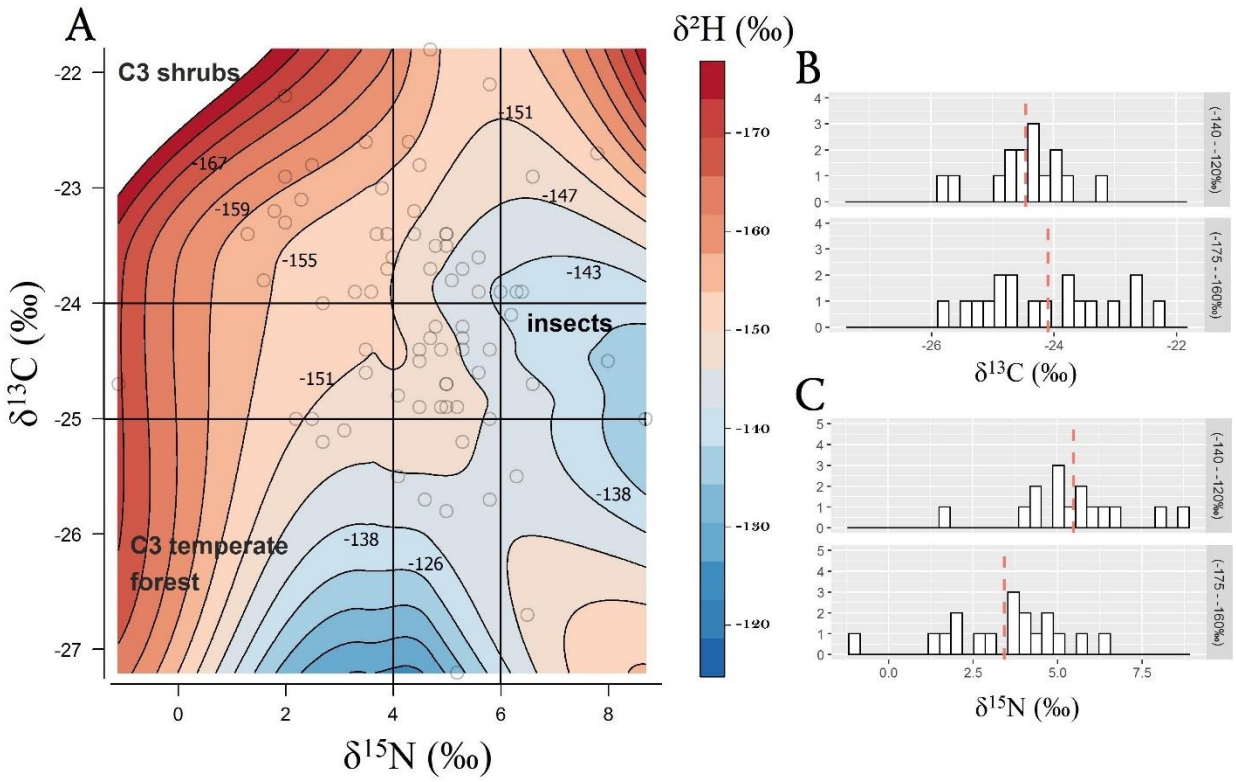

Figure 6. Isotopic diet composition of $\delta^{13}C$ and $\delta^{15}N$ plotted over $\delta^{2}H$ spatial data distribution (panel A). Blue areas represent lower latitudes of origin ($\delta^{2}H$ = from -110‰ to -145‰) while red areas represent higher latitudes of origin ($\delta^{2}H$ = from -145‰ to -180‰). Each open circle represents a single individual. Northern migrants show a moderate trend towards lower protein consumption ($\delta^{15}N$: 1-4‰) and C3-plant habitat use ($\delta^{13}C$: -22 – -24‰). Southern migrants show higher trophic level ($\delta^{15}N$: 4-8‰) and temperate forests habitat use ($\delta^{13}C$: -24 – -26‰). Panels B and C show the distributions of $\delta^{13}C$ and $\delta^{15}N$ values across migrants originating from extreme northern and extreme southern latitudes. Dashed red lines represent isotope mean values for each group.

Discussion

Bridge et al. (2010) conducted a captive experiment in which wintering Dark-eyed Juncos were fed *ad libitum* to demonstrate that fat depositions allow them to initiate migration earlier in the spring compared to the control group. We extended previous work by providing a geostatistical approach illustrating the explicit spatial distribution of breeding and molting origin of fall migrants and related that distribution to morphological characteristics and trophic level differentiation. Our geographical assignments clearly suggested that migratory juncos wintering in central Oklahoma originated from different breeding and molting areas (Fig 3 and suppl. material S1-S4). We identified northern and southern migrants while each group also showed intra-cohort spatial variation ranging from Alaska and western Canada to central Northwestern Territories, and Northern Saskatchewan to southern Manitoba and northwestern United States, respectively. However, despite the posterior probability surfaces showing population admixture at the wintering area in Oklahoma, our modeling effort showed no association between winter body condition and breeding or molting latitude.

Stable isotope ratios of hydrogen, carbon, and nitrogen, extracted from inert animal tissues, such as claws and feathers, reflect the isotope ratios in the environment where those tissues were grown and can provide inferences about large-scale animal movements and diet preferences in species with small body size (Rubenstein and Hobson, 2004; Zenzal et al., 2018; Vander Zanden et al., 2018). However, a clear advantage of adopting a multi-element stable isotope approach is that migrants can be assigned to different breeding and molting grounds of origin while their diet preferences are also revealed and clustered in trophic guilds (Herrera et al., 2003). The positive correlation between nitrogen ($\delta^{15}N$) and hydrogen ($\delta^{2}H$) values, although moderate, corroborated our hypothesis that wintering birds originating from northern latitudes

would have lower protein intake relative to southern migrants and prefer a diet rich in carbohydrates before migrating. That is, increased carbohydrate anabolism and lower protein consumption is necessary to quickly synthesize enough subcutaneous lipid reserves to sustain a long-distance migration (Cecere, et al., 2011; Domer et al., 2018). Alternatively, higher $\delta^{15}N$ values in southern migrants might be explained by environmental stressors. An early study in captive quails (*Coturnix japonica*) and geese (*Anser rossii*) showed that increased $\delta^{15}N$ values can be obtained from growing tissues of individuals maintained under severe nutritional stress conditions (e.g., fasting) compared to control groups (Hobson et al. 1993). However, subsequent analysis in sparrows (*Melospiza melodia*) found no differences in $\delta^{15}N$ between birds kept under a restricted diet versus birds fed *ad libitum* (Kempster et al., 2007) suggesting a less straightforward relationship between physiological stress conditions and $\delta^{15}N$ values. Therefore, even though we cannot pinpoint the exact causes of increased $\delta^{15}N$ values in growing feathers (e.g., baseline difference) and that other species have shown variation in feather $\delta^{15}N$ values between boreal and more southern food webs based on land use (Hobson 1999), it is also possible that migratory juncos originating from southern latitudes were foraging at a higher level in the trophic system and consuming more insects compared to northern migrants. We do not exclude that such diet preference might be linked to an opportunistic foraging strategy due to an outburst of insect availability (Yang et al., 2008). However, analysis of isotopic niche shifts in avian migratory populations have shown sharp changes during different life cycle stages (Hahn, et al., 2013), confirming that variations in diet compositions have a defined role in maintaining fluctuating energy needs (Marshall et al., 2016). Moreover, our $\delta^{13}C$ results indicated that northern juncos might exploit food resources from a broader range of habitats compared to southern juncos, ranging from pine forest to deciduous forest (e.g., oak) and C3 shrubs. Bearhop

et al. (2004) studied the Thick-billed Vireos (*Vireo crassirostris*) in the Bahamas and based on mean claw $\delta^{13}C$ values found differences among two groups of birds occupying environments with either prevalent xerophytic shrubs or pine forest. While our feather $\delta^{13}C$ results showed that northern juncos seed consumption fell within the spectrum of plants characterized by a C3 photosynthetic pathway, and we found enough variation to highlight habitat occupancy differentiations across latitudinal origins (Fig 5 and Fig 6), we note that a robust environmental isotopic baseline is necessary to determine dietary and habitat preferences with confidence (Post, 2002).

The interactions between avian body mass fluctuations and migratory behaviors within and between seasons remain poorly understood (Brown and Sherry, 2006; Tsvey et al., 2007; Marra et al. 2015). Importantly, body condition appears to both influence and be influenced by migratory behavior. For example, body condition may affect migratory decisions (Schaub and Jenni 2000); several species of migrating shorebirds underwent longer migratory flights when departing with higher body condition scores (Anderson et al. 2019). Similarly, spring arrival timing of red knots (*Calidris canutus*) was associated with better body condition at a major stopover site (Duijns et al. 2017) and conditions experienced during winter months by American Redstarts (*Setophaga ruticilla*) lead to variation in body conditions that predicted spring departure dates (Marra et al., 1998). In our study, individuals that migrated minimum distances did non exhibit larger body masses or higher fat scores over the early winter period. However, an ideal capturing effort occurring immediately upon arrival in Oklahoma might reveal mass as a predictor of latitude of origin because the body condition of those migrants would provide a stronger indication of the migration strategy performed. Moreover, there may be other mechanisms that could explain the absence of a relationship between body conditions and

migration strategies in our study population. For example, the taxonomy of the genus junco has been challenging for decades and is far from being resolved (Miller 1941; Nolan et al., 2002; Aleixandre et al., 2013). The species *Junco hyemalis* has been recently proposed to be phylogenetically reassessed based on extensive genomic data to determine if it needs to be split into four new species that also account for distinct phenotypic variation (Friis et al., 2016). Thus, in a complex migratory system, it is possible that in some populations different morphs of migrants characterized by a larger and smaller than average body size could come into contact at the winter ground and therefore confounding the effects of energy consumption during migration. Alternatively, long distance migrants could also improve their body conditions (e.g., increase mass at stopover sites) before arriving at their final wintering destination and reduce the difference in body mass compared to short distance migrants. However, if the stopover site is only used to refuel without growing new feathers, the stable isotope analysis will still detect the northern origin (e.g., molting ground) and correctly identify the migration latitudinal origin without revealing any geographical information on the stopover location.

Conclusions

By implementing a Bayesian assignment framework, we offered a probabilistic geographic explanation of the junco's feather isotopic variation across the species' breeding and molting areas in the northern hemisphere and generated a set of competing hypotheses to explain latitudinal origin in relation to morphological traits (Wunder, 2010; Maggini et al., 2016). In our system, none of the variables considered had a clear effect on feather hydrogen stable isotope values (used as a proxy for latitudinal origin) although we found indication of a possible higher trophic level shift in individuals migrating from southern latitudes. These findings promote the concurrent use of different stable isotope markers as a means of studying interconnected

behavioral traits. Our results also highlight the need to carefully examine confounding effects in explanatory models in relation to the species' natural history and possible differential migratory behaviors across populations.

Abbreviations

NRMN: Norman; AICc: Akaike Information Criterion corrected for small sample sizes; G1: Group 1; G2: Group 2; G3: Group 3; G4: Group 4.

Consent for publication

Not applicable.

Availability of data and materials

Additional datasets used and/or analyzed in the current study are available from the corresponding author on reasonable request.

Competing interests

The authors have no competing interests.

Funding

AC was supported by NSF grant DBI-1565128**;** JFK and ESB were supported by NSF grants DGE-1545261 and EF-1840230.

Authors' contributions

AC conceptualized the project, analyzed the data, and wrote the manuscript. AKP analyzed the data, reviewed, and edited the manuscript. SWY provided key feedback on data analysis, reviewed, and edited the manuscript. ESB collected the data and reviewed the manuscript. JFK collected the data and reviewed the manuscript. MBW supervised data analysis and reviewed the manuscript.

Acknowledgments

We thank the researchers at the Oklahoma Biological Survey and University of Oklahoma for collecting and analyzing the feather samples used in this study. We also thank Vojtěch Brlík for his constructive comments, which helped us to improve the first draft of the manuscript.

References

Alerstam, T., 2011. Optimal bird migration revisited. *Journal of Ornithology*, *152*(1), pp.5-23.

Alerstam, T. and Bäckman, J., 2018. Ecology of animal migration. *Current Biology*, *28*(17), pp.R968-R972.

Anderson, A. M., S. Duijns, P. A. Smith, C. Friis, and E. Nol. 2019. Migration Distance and Body Condition Influence Shorebird Migration Strategies and Stopover Decisions During Southbound Migration. Frontiers Ecol Evol 7:251.

Arcese, Peter, Mark K. Sogge, Amy B. Marr and Michael A. Patten. (2002). Song Sparrow (*Melospiza melodia*), version 2.0. In The Birds of North America (P. G. Rodewald, editor). Cornell Lab of Ornithology, Ithaca, New York, USA.

Barton, K. and Barton, M.K., 2019. Package 'MuMIn'. *Multi-model inference. version*, *1*(6).

Bearhop, S., Hilton, G.M., Votier, S.C. and Waldron, S., 2004. Stable isotope ratios indicate that body condition in migrating passerines is influenced by winter habitat. *Proceedings of the Royal Society of London. Series B: Biological Sciences*, *271*(suppl_4), pp.S215-S218.

BirdLife International and Handbook of the Birds of the World (2016) Bird species distribution maps of the world". Version 6.0. Available at http://datazone.birdlife.org/species/requestdis.

Bridge, E.S., Kelly, J.F., Bjornen, P.E., Curry, C.M., Crawford, P.H. and Paritte, J.M., 2010. Effects of nutritional condition on spring migration: do migrants use resource availability to keep pace with a changing world? *Journal of Experimental Biology*, *213*(14), pp.2424-2429.

Brown, D.R. and Sherry, T.W., 2006. Food supply controls the body condition of a migrant bird wintering in the tropics. *Oecologia*, *149*(1), pp.22-32.

Cecere, J.G., Spina, F., Jenni-Eiermann, S. and Boitani, L., 2011. Nectar: an energy drink used by European songbirds during spring migration. *Journal of Ornithology*, *152*(4), pp.923-931.

Cooper, N.W., Sherry, T.W. and Marra, P.P., 2015. Experimental reduction of winter food decreases body condition and delays migration in a long-distance migratory bird. *Ecology*, *96*(7), pp.1933-1942.

DeLuca, W.V., Woodworth, B.K., Rimmer, C.C., Marra, P.P., Taylor, P.D., McFarland, K.P., Mackenzie, S.A. and Norris, D.R., 2015. Transoceanic migration by a 12 g songbird. *Biology letters*, *11*(4), p.20141045.

Domer, A., Ovadia, O. and Shochat, E., 2018. Energy for the road: Influence of carbohydrate and water availability on fueling processes in autumn-migrating passerines. The Auk: Ornithological Advances, 135(3), pp.534-546.

Duijns, S., L. J. Niles, A. Dey, Y. Aubry, C. Friis, S. Koch, A. M. Anderson, and P. A. Smith. 2017. Body condition explains migratory performance of a long-distance migrant. Proc Royal Soc B 284:20171374.

Fudickar, A.M., Greives, T.J., Atwell, J.W., Stricker, C.A. and Ketterson, E.D., 2016. Reproductive allochrony in seasonally sympatric populations maintained by differential response to photoperiod: implications for population divergence and response to climate change. *The American Naturalist*, *187*(4), pp.436-446.

Green, A.J., 2001. Mass/length residuals: measures of body condition or generators of spurious results? *Ecology*, *82*(5), pp.1473-1483.

Guglielmo, C.G., 2018. Obese super athletes: fat-fueled migration in birds and bats. *Journal of Experimental Biology*, *221*(Suppl 1), p.jeb165753.

Hahn, S., Amrhein, V., Zehtindijev, P. and Liechti, F., 2013. Strong migratory connectivity and seasonally shifting isotopic niches in geographically separated populations of a long-distance migrating songbird. Oecologia, 173(4), pp.1217-1225.

Helms, C.W. and Drury, W.H., 1960. Winter and migratory weight and fat field studies on some North American buntings. *Bird-banding*, *31*(1), pp.1-40.

Herrera, L.G., Hobson, K.A., Rodríguez, M. and Hernandez, P., 2003. Trophic partitioning in tropical rain forest birds: insights from stable isotope analysis. Oecologia, 136(3), pp.439-444.

Hobson, K.A., Alisauskas, R.T. and Clark, R.G., 1993. Stable-nitrogen isotope enrichment in avian tissues due to fasting and nutritional stress: implications for isotopic analyses of diet. *The Condor*, *95*(2), pp.388-394.

Hobson, K.A. and Wassenaar, L.I., 1996. Linking breeding and wintering grounds of neotropical migrant songbirds using stable hydrogen isotopic analysis of feathers. *Oecologia*, *109*(1), pp.142-148.

Hobson, K.A., 1999. Stable-carbon and nitrogen isotope ratios of songbird feathers grown in two terrestrial biomes: implications for evaluating trophic relationships and breeding origins. The Condor, 101(4), pp.799-805.

Hobson, K.A., Van Wilgenburg, S.L., Wassenaar, L.I. and Larson, K., 2012. Linking hydrogen (δ2H) isotopes in feathers and precipitation: sources of variance and consequences for assignment to isoscapes. *PloS one*, *7*(4), p.e35137.

Hobson, K.A. and Koehler, G., 2015. On the use of stable oxygen isotope (δ18O) measurements for tracking avian movements in North America. *Ecology and Evolution*, *5*(3), pp.799-806.

Horton, K.G., Van Doren, B.M., Stepanian, P.M., Farnsworth, A. and Kelly, J.F., 2016. Seasonal differences in landbird migration strategies. *The Auk: Ornithological Advances*, *133*(4), pp.761-769.

Kaboli, M., Aliabadian, M., Guillaumet, A., Roselaar, C.S. and Prodon, R., 2007. Ecomorphology of the wheatears (genus Oenanthe). *Ibis*, *149*(4), pp.792-805.

Keeley, J.E. and Rundel, P.W., 2003. Evolution of CAM and C4 carbon-concentrating mechanisms. *International Journal of Plant Sciences*, *164*(S3), pp.S55-S77.

Kelly, J.F., Bridge, E.S., Fudickar, A.M. and Wassenaar, L.I., 2009. A test of comparative equilibration for determining non-exchangeable stable hydrogen isotope values in complex organic materials. Rapid Communications in Mass Spectrometry: An International Journal Devoted to the Rapid Dissemination of Up-to-the-Minute Research in Mass Spectrometry, 23(15), pp.2316-2320.

Kempster, B., Zanette, L., Longstaffe, F.J., MacDougall-Shackleton, S.A., Wingfield, J.C. and Clinchy, M., 2007. Do stable isotopes reflect nutritional stress? Results from a laboratory experiment on song sparrows. *Oecologia*, *151*(3), pp.365-371.

Liebgold, E.B., Gerlach, N.M. and Ketterson, E.D., 2019. Density-dependent fitness, not dispersal movements, drives temporal variation in spatial genetic structure in dark-eyed juncos (*Junco hyemalis*). *Molecular ecology*, *28*(5), pp.968-979.

Ma, C., Vander Zanden, H.B., Wunder, M.B. and Bowen, G.J., 2020. assignR: An R package for isotope-based geographic assignment. *Methods in Ecology and Evolution*.

Maggini, I., Metzger, B., Voss, M., Voigt, C.C. and Bairlein, F., 2016. Morphometrics and stable isotopes differentiate wintering populations of a migratory bird. *Movement ecology*, *4*(1), p.20.

Marra, P. P., E. B. Cohen, S. R. Loss, J. E. Rutter, and C. M. Tonra. 2015. A call for full annual cycle research in animal ecology. Biol Letters 11:20150552.

Marra, P. P., K. A. Hobson, and R. T. Holmes. 1998. Linking winter and summer events in a migratory bird by using stable-carbon isotopes. Science 282:1884–1886.

Marshall, T.J., Dick, M.F. and Guglielmo, C.G., 2016. Seasonal dietary shifting in yellow-rumped warblers is unrelated to macronutrient targets. *Comparative Biochemistry and Physiology Part A: Molecular & Integrative Physiology*, *192*, pp.57-63.

Nolan, V., Jr, and E. D. Ketterson. 1983. An analysis of body mass, wing length, and visible fat deposits of Dark-eyed Juncos wintering at different latitudes. The Wilson bulletin.

Nolan, V., Jr, Ketterson, E. D., Cristol, D. A., Rogers, C. M., Clotfelter, E. D., Titus, R. C., Schoech, S. J., Snajdr, E, 2002. Dark-eyed Junco (*Junco hyemalis*), version 2.0. In The Birds of North America (A. F. Poole and F. B. Gill, Editors). Cornell Lab of Ornithology, Ithaca, NY, USA. https://doi.org/10.2173/bna.716

Paritte, J.M. and Kelly, J.F., 2009. Effect of cleaning regime on stable-isotope ratios of feathers in Japanese Quail (*Coturnix japonica*). *The Auk*, *126*(1), pp.165-174.

PIF (Partners in Flight), 2017. Avian Conservation Assessment Database, version 2017. http://pif.birdconservancy.org.

Post, D.M., 2002. Using stable isotopes to estimate trophic position: models, methods, and assumptions. Ecology, 83(3), pp.703-718.

R Core Team (2020) R: A Language and Environment for Statistical Computing. R Foundation for Statistical Computing, Vienna, Austria. Available: http://www.r-project.org.

Rani, S., Singh, S., Malik, S. and Kumar, V., 2017. Insights into the Regulation of Spring Migration in Songbirds. In *Biological Timekeeping: Clocks, Rhythms and Behaviour* (pp. 625-642). Springer, New Delhi.

Reif, J., Hořák, D., Krištín, A., Kopsová, L. and Devictor, V., 2016. Linking habitat specialization with species' traits in European birds. *Oikos*, *125*(3), pp.405-413.

Revelle, W. and Revelle, M.W., 2015. Package ‘psych’. *The comprehensive R archive network*.

Rogers, C.M., Nolan, V. and Ketterson, E.D., 1994. Winter fattening in the dark-eyed junco: plasticity and possible interaction with migration trade-offs. *Oecologia*, *97*(4), pp.526-532.

Rubenstein, D. R. and K. A. Hobson. 2004. From birds to butterflies: animal movement patterns and stable isotopes. *Trends in Ecology and Evolution* 19(5): 256-263.

Tsvey, A., Bulyuk, V.N. and Kosarev, V., 2007. Influence of body condition and weather on departures of first-year European robins, Erithacus rubecula, from an autumn migratory stopover site. *Behavioral Ecology and Sociobiology*, *61*(11), pp.1665-1674.

Sarkar, D., 2008. The Lattice Package: Lattice Graphics. R package Version 0.17-15. *URL: http://cran. r-project. org/web/packages/lattice/index. html*.

Schaub, M., and L. Jenni. 2000. Body mass of six long-distance migrant passerine species along the autumn migration route. J Für Ornithol 141:441–460.

Vander Zanden, H.B., Nelson, D.M., Wunder, M.B., Conkling, T.J. and Katzner, T., 2018. Application of isoscapes to determine geographic origin of terrestrial wildlife for conservation and management. *Biological Conservation*, *228*, pp.268-280.

Wassenaar, L.I. and Hobson, K.A., 2003. Comparative equilibration and online technique for determination of non-exchangeable hydrogen of keratins for use in animal migration studies. Isotopes in environmental and health studies, 39(3), pp.211-217.

Wassenaar, L.I. and Hobson, K.A., 2006. Stable-hydrogen isotope heterogeneity in keratinous materials: mass spectrometry and migratory wildlife tissue subsampling strategies. *Rapid Communications in Mass Spectrometry: An International Journal Devoted to the Rapid Dissemination of Up-to-the-Minute Research in Mass Spectrometry*, *20*(16), pp.2505-2510.

Wunder, M.B., 2010. Using isoscapes to model probability surfaces for determining geographic origins. In *Isoscapes* (pp. 251-270). Springer, Dordrecht.

Yanco, S.W., McDevitt, A., Trueman, C.N., Hartley, L. and Wunder, M.B., 2020. A modern method of multiple working hypotheses to improve inference in ecology. *Royal Society Open Science*, *7*(6), p.200231.

Yang, L.H., Bastow, J.L., Spence, K.O. and Wright, A.N., 2008. What can we learn from resource pulses. *Ecology*, *89*(3), pp.621-634.

Zenzal, T.J., Contina, A.J., Kelly, J.F. and Moore, F.R., 2018. Temporal migration patterns between natal locations of ruby-throated hummingbirds (*Archilochus colubris*) and their Gulf Coast stopover site. *Movement ecology*, *6*(1), p.2.

Supplementary Material

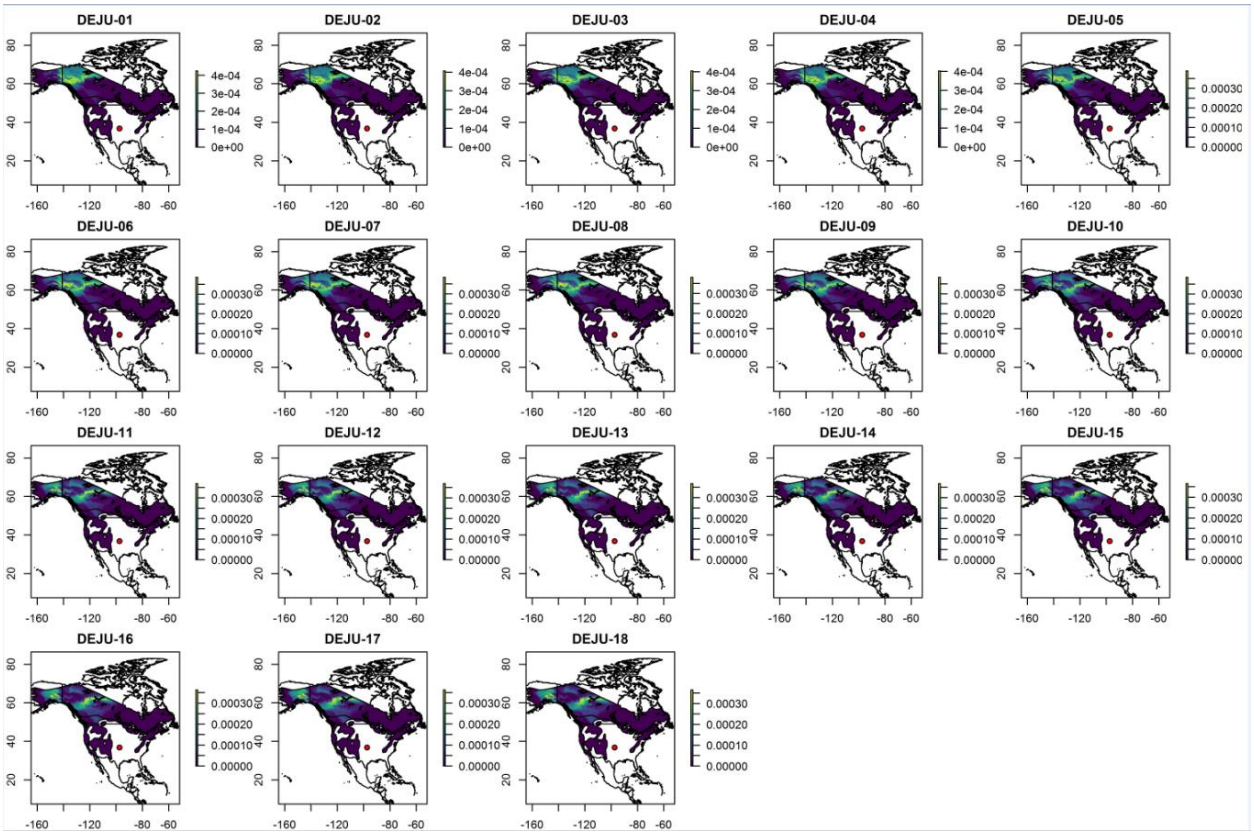

Figure S1. Individual posterior probability assignment maps for group G1 (high depleted) including δ^2H_f values ranging from -175.6‰ to -160.2‰ (M = -167.1‰, SD = 5.02‰, N = 18).

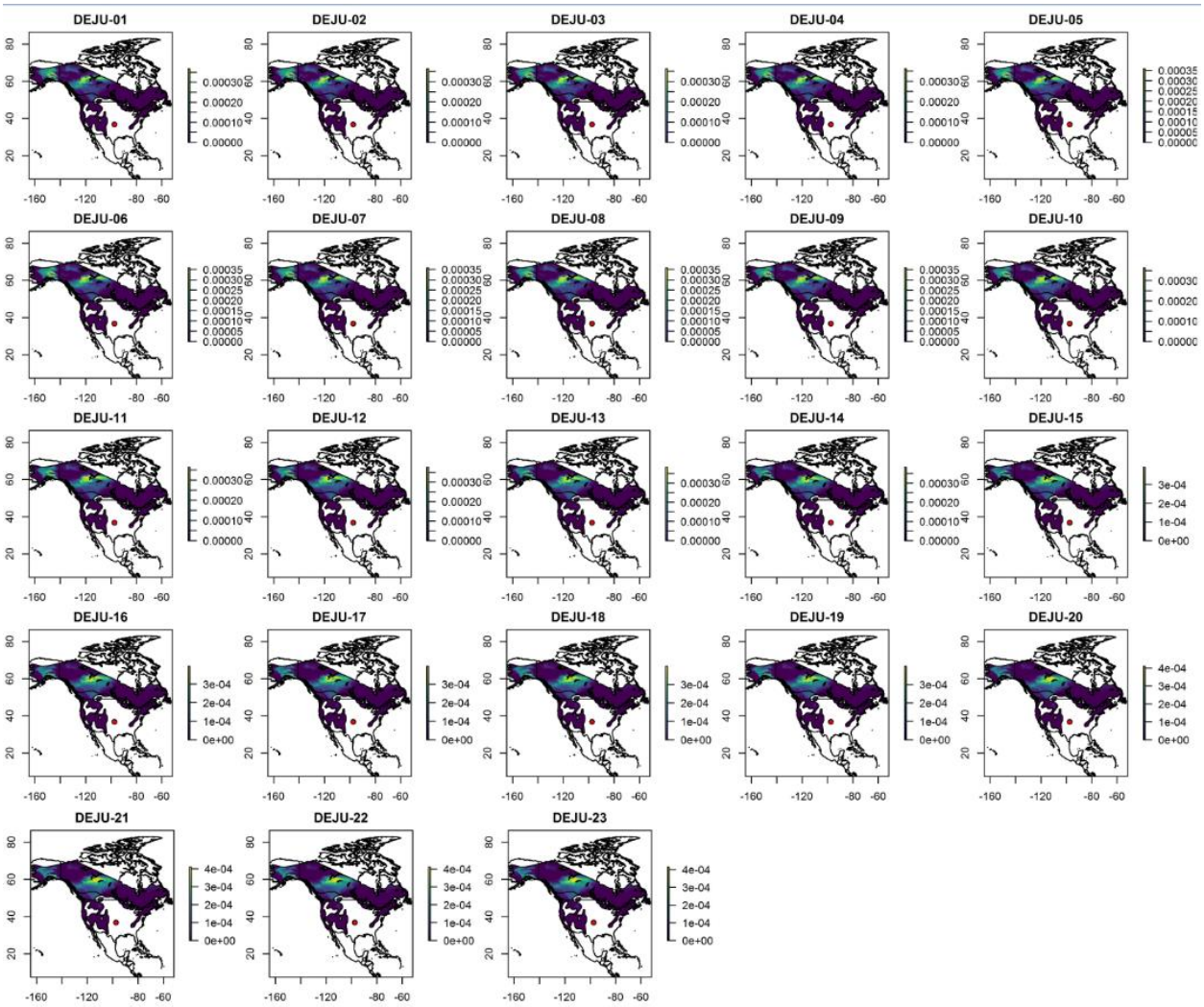

Figure S2. Individual posterior probability assignment maps for group G2 (low depleted) including δ^2H_f values ranging from -159.3‰ to -150.4‰ (M = -154.9‰, SD 3.17‰, N = 23).

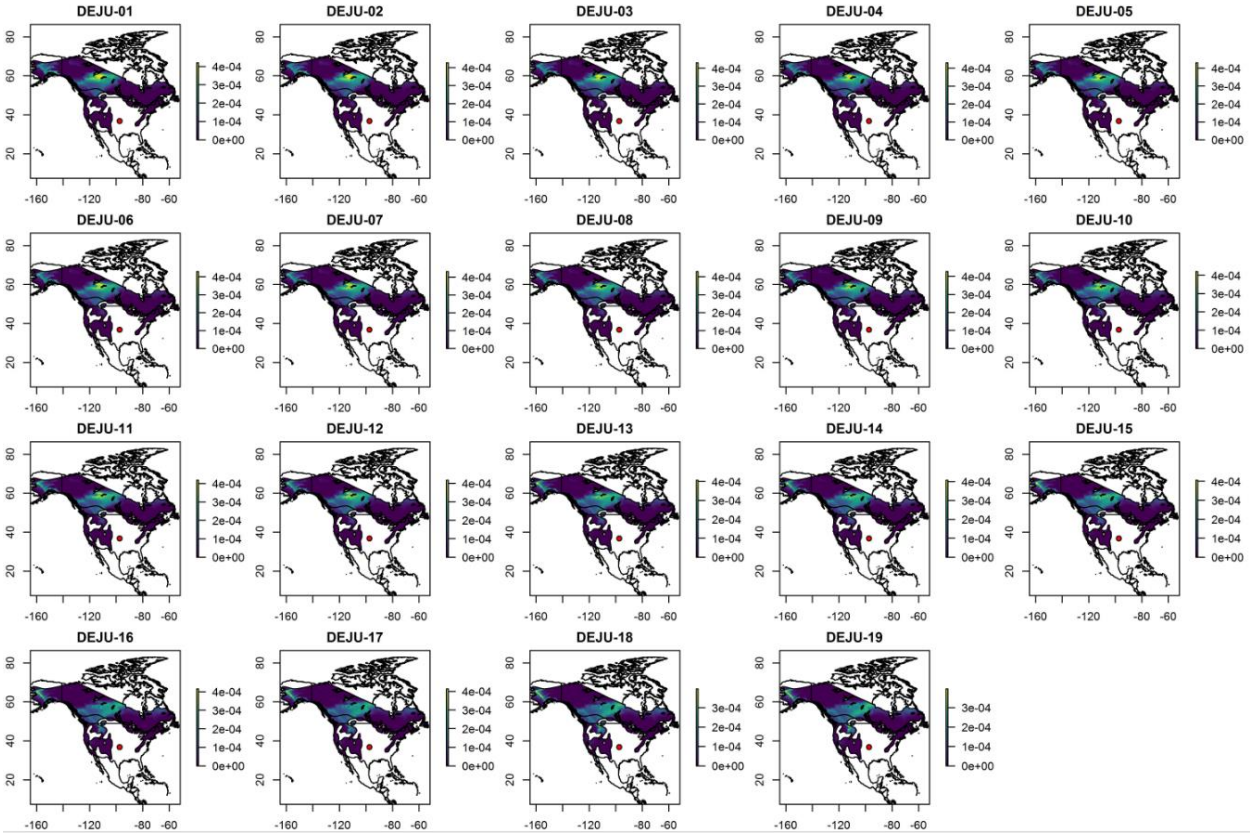

Figure S3. Individual posterior probability assignment maps for group G3 (low enriched) including δ^2H_f values ranging from -149.8‰ to -140.1‰ (M = -145.4‰, SD = 2.88‰, N = 19).

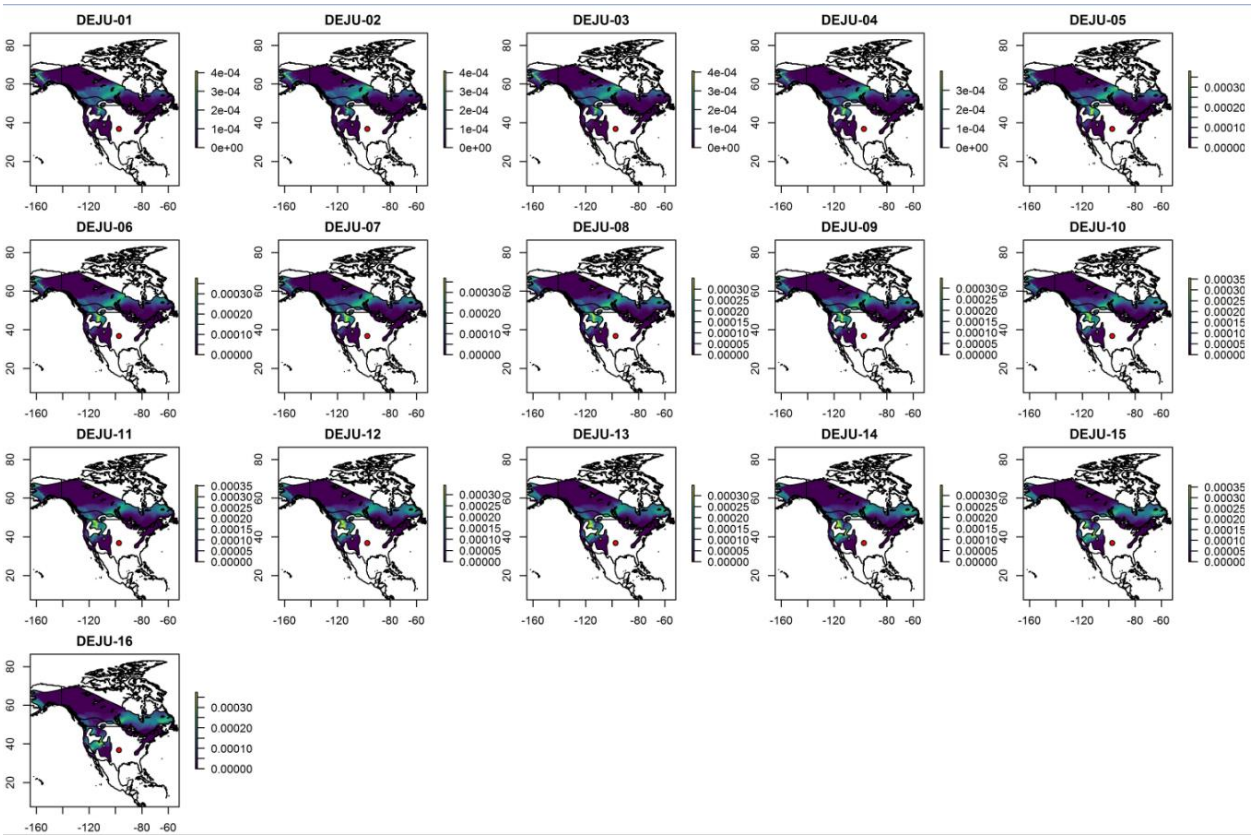

Figure S4. Individual posterior probability assignment maps for group G4 (high enriched) including δ^2H_f values ranging from -139.3‰ to -118.6‰ (M = -130.4‰, SD = 6.39‰, N = 16).

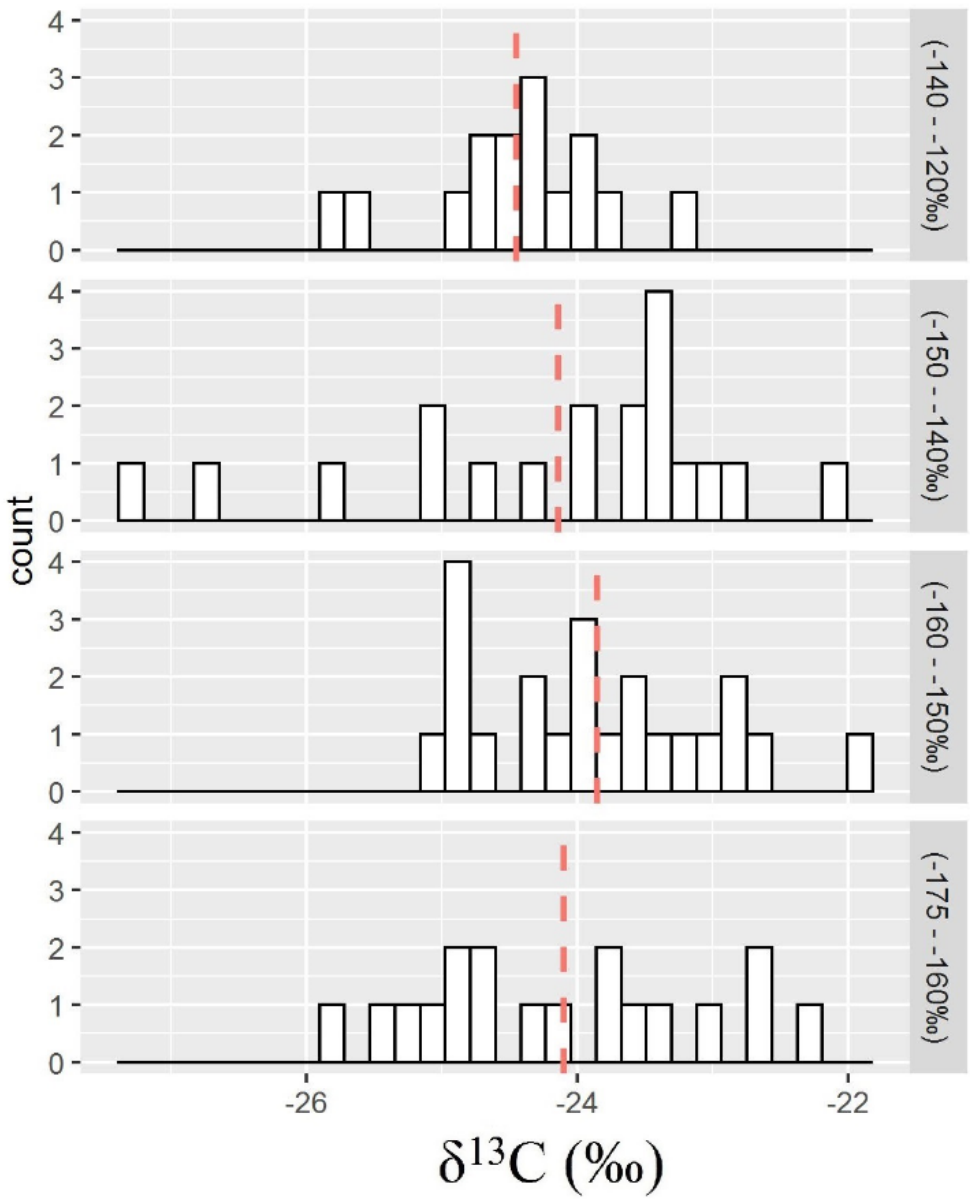

Figure S5. Distributions of $\delta^{13}C$ values across migrants originating across latitudinal groups. Dashed red lines represent stable isotope mean values for each group.

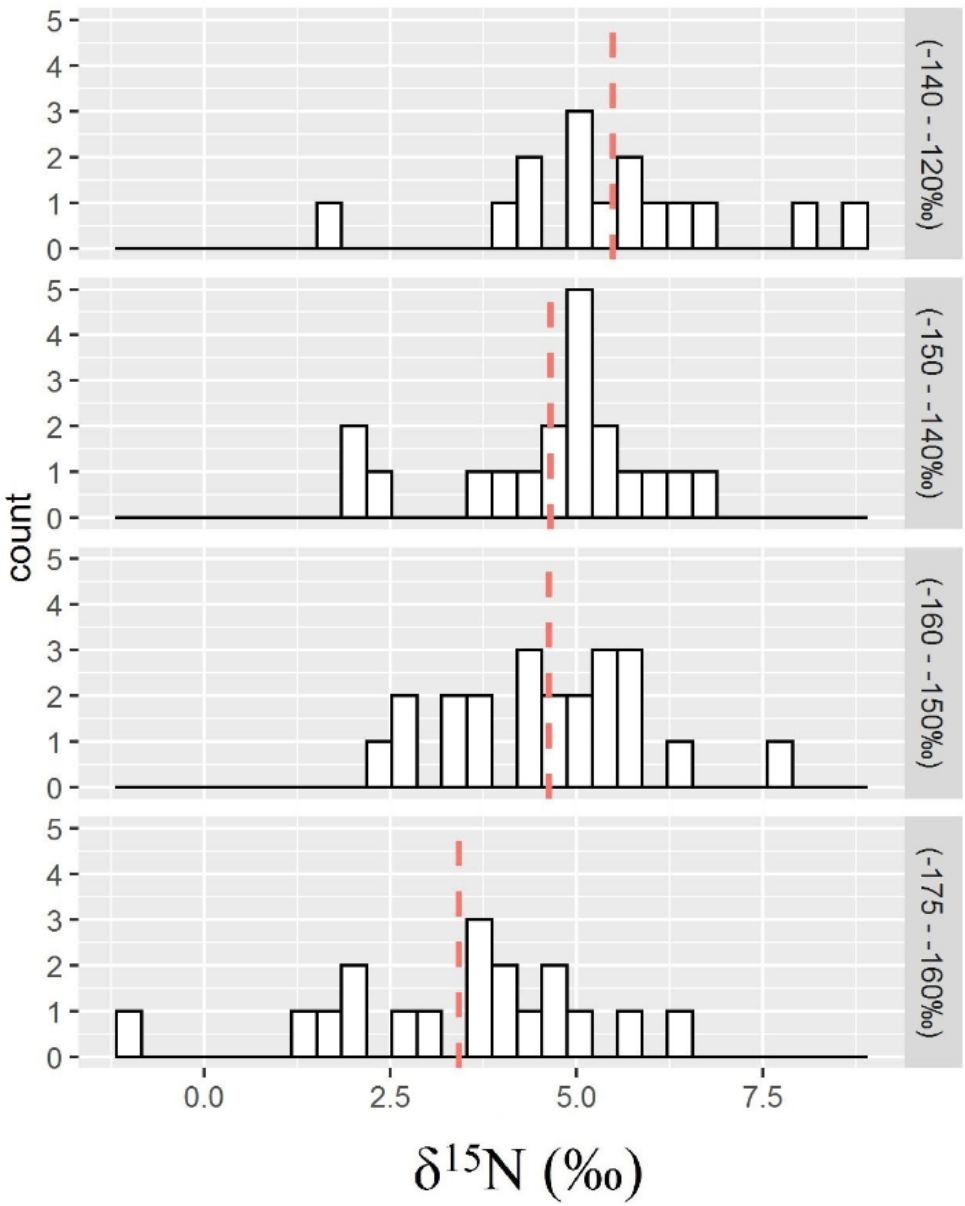

Figure S6. Distributions of $\delta^{15}N$ values across migrants originating across latitudinal groups. Dashed red lines represent stable isotope mean values for each group.

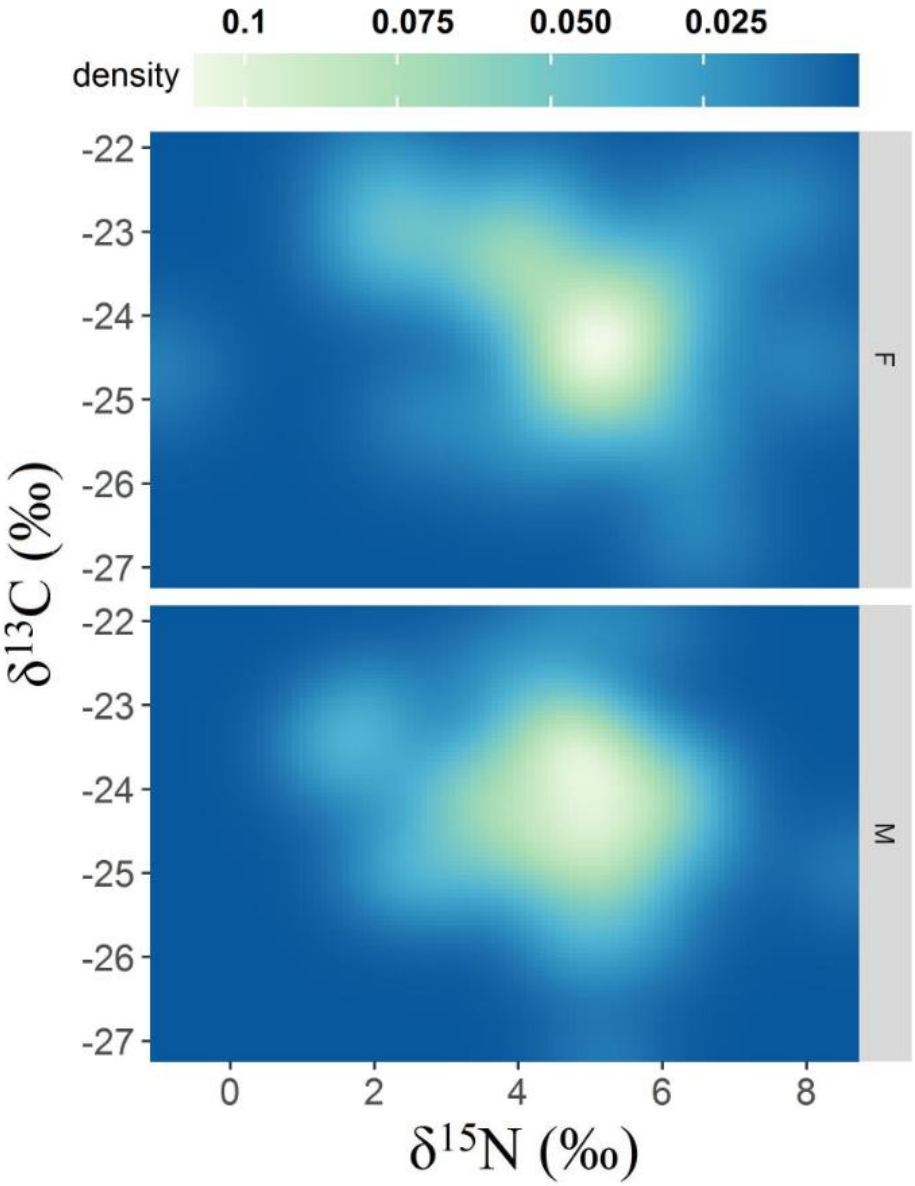

Figure S7. Diet niche and food preferences between males (M) and females (F). Males show a slightly larger dietary niche compared to females but no substantial differences.

Supplementary Tables

	TEMP.AVG (°C)	TEMP.MN (°C)	TEMP.MAX (°C)	RAIN.AVG (mm)	HUMID.MIN (%)	HUMID.MAX (%)	WIND.AVG (kph)
December	4	-12.2	24.4	24.6	13	98	15.2
January	2.7	-12.2	26.1	22.8	11	98	12
February	8.9	-6.6	26.6	23.6	15	97	32.3
Winter.AVG	5.2	-10.5	25.7	23.6	13	97.6	19.8

Table S1. Details of the weather conditions experienced by the Dark-eyed Juncos wintering in central Oklahoma between December 2008 through February 2009 and recorded by the Oklahoma Climatological Survey and the Oklahoma Mesonet (www.mesonet.org) program at the Norman (NRMN) weather station. Wind data are relative to the number of days with average wind speed ≥ 16 kph. This weather station was the nearest to the study site.

Model	Intercept		Fat2		Fat3		Fat4		Fat5		Mass		Tail		Tarsus		Wing		df	logLik	AICc	delta	weight
	ß	SE	ß	SE	ß	SE	ß	SE	ß	SE	ß	SE	ß	SE	ß	SE	ß	SE					
32	-144.95	6.93	-4.42	5.74	-7.74	5.8	-6.9	6.11	-1.87	13.63	4.81	2.74	-2.97	3.23	-0.93	1.83	6.77	3.83	51	-222.1	471.48	0	0.3
24	-145.43	6.59	-4.18	5.68	-7.11	5.65	-6.46	5.99	-1.56	13.53	4.43	2.65	-2.93	3.21			6.37	3.75	52	-223.74	471.8	0.33	0.25
28	-145.31	6.85	-3.97	5.71	-7.26	5.78	-6.66	6.09	-3.27	13.53	4.3	2.69			-0.88	1.82	4.49	2.95	52	-224.61	473.54	2.06	0.11
20	-145.76	6.52	-3.75	5.65	-6.67	5.62	-6.25	5.97	-2.96	13.43	3.95	2.59					4.15	2.87	53	-226.25	473.95	2.47	0.09
30	-144.56	5.7	-6.46	5.77	-7.76	5.93	-8.22	6.21	-2.69	13.94			-1.91	3.24	-0.08	1.81	7.4	3.65	52	-225.43	475.16	3.69	0.05
22	-144.61	5.56	-6.42	5.65	-7.7	5.74	-8.16	6.03	-2.64	13.79			-1.92	3.21			7.36	3.53	53	-226.94	475.33	3.86	0.04
16	-146.85	5.19	-3.42	5.72	-5.35	5.78	-7.09	6.18	-4.09	13.94	5.1	2.58	0.09	2.46	-0.27	1.84			52	-225.65	475.61	4.13	0.04
8	-146.96	5.05	-3.39	5.64	-5.2	5.64	-6.97	6.03	-3.97	13.78	4.96	2.46	0.04	2.43					53	-227.18	475.83	4.35	0.03
12	-146.84	5.03	-3.54	5.64	-5.36	5.71	-7.21	6.12	-4.17	13.74	4.98	2			-0.25	1.82			53	-227.46	476.38	4.91	0.03
4	-146.94	4.92	-3.5	5.57	-5.23	5.57	-7.09	5.97	-4.08	13.59	4.85	1.81							54	-228.98	476.68	5.21	0.02
26	-144.83	5.7	-6.02	5.69	-7.44	5.87	-7.96	6.16	-3.56	13.77					-0.11	1.8	5.84	2.41	53	-227.69	476.85	5.37	0.02
18	-144.89	5.55	-5.96	5.57	-7.36	5.67	-7.89	5.98	-3.51	13.62							5.79	2.24	54	-229.2	477.11	5.63	0.02
14	-146.66	5.07	-4.68	5.81	-4.96	5.93	-7.49	6.3	-4.41	14.29			2.89	1.83	0.69	1.82			53	-229.25	479.96	8.48	0
6	-146.34	4.96	-4.96	5.72	-5.36	5.79	-7.95	6.14	-4.84	14.14			3.12	1.71					54	-230.84	480.39	8.91	0
10	-147.59	5.1	-4.03	5.87	-3.42	5.93	-6.78	6.37	-0.89	14.31					1.65	1.74			54	-232.01	482.74	11.26	0
31	-150.54	4.62									4.64	2.61	-2.55	3.13	-0.29	1.75	5.58	3.57	55	-233.91	483.9	12.42	0
2	-146.87	5.11	-4.8	5.83	-4.27	5.86	-8.03	6.27	-1.7	14.29									55	-233.92	483.91	12.44	0
23	-150.57	4.51									4.52	2.52	-2.54	3.1			5.48	3.51	56	-235.4	484.32	12.85	0
27	-150.55	4.59									4.16	2.54			-0.27	1.74	3.72	2.75	56	-236.3	486.13	14.66	0
19	-150.57	4.49									4.06	2.45					3.64	2.69	57	-237.79	486.64	15.16	0
15	-151.19	2.51									5.07	2.49	0.12	2.4	0.17	1.76			56	-237.14	487.81	16.33	0
29	-151.03	3.07											-1.38	3.12	0.51	1.73	6.41	3.42	56	-237.26	488.04	16.56	0
7	-151.18	2.54									5.15	2.39	0.16	2.37					57	-238.62	488.32	16.84	0
21	-150.98	3.17											-1.34	3.09			6.67	3.35	57	-238.76	488.6	17.12	0
11	-151.24	2.32									5.02	1.97			0.19	1.74			57	-238.93	488.93	17.45	0
3	-151.22	2.35									5.14	1.82							58	-240.4	489.51	18.03	0
25	-151	3.14													0.47	1.72	5.33	2.23	57	-239.41	489.89	18.41	0
17	-150.96	3.24															5.6	2.12	58	-240.9	490.51	19.03	0
13	-151.49	1.64											2.73	1.74	1.11	1.74			57	-240.75	492.58	21.1	0
5	-151.49	1.63											3.08	1.64					58	-242.43	493.56	22.09	0
9	-151.49	1.66													1.98	1.67			58	-243.45	495.6	24.13	0
1	-151.49	1.66																	59	-245.58	497.58	26.1	0

Table S2. Akaike Information Criterion corrected for small sample size (AICc) model results. The table shows the full list of the 32 ranked models.